

Comparison of multi-recognition molecularly imprinted polymers for recognition of melamine, cyromazine, triamterene, and trimethoprim

Xian-Hua Wang¹ · Jing Zhang¹ · Chao Peng¹ · Qian Dong¹ · Yan-Ping Huang¹ · Zhao-Sheng Liu¹

Received: 3 April 2015 / Revised: 5 June 2015 / Accepted: 23 June 2015 / Published online: 21 July 2015
© Springer-Verlag Berlin Heidelberg 2015

Abstract Three fragmental templates, including 2,4-diamino-6-methyl-1,3,5-triazine (DMT), cyromazine (CYR), and trimethoprim (TME), were used to prepare the fragment molecularly imprinted polymers (FMIPs), respectively, in polar ternary porogen which was composed of ionic liquid ([BMIM]BF₄), methanol, and water. The morphology, specific surface areas, and selectivity of the obtained FMIPs for fragmental analogues were systematically characterized. The experimental results showed that the FMIPs possessed the best specific recognition ability to the relative template and the greatest imprinting factor (IF) was 5.25, 6.69, and 7.11 of DMT on DMT-MIPs, CYR on CYR-MIPs, and TME on TME-MIPs, respectively. In addition, DMT-MIPs also showed excellent recognition capability for fragmental analogues including CYR, melamine (MEL), triamterene (TAT), and TME, and the IFs were 2.08, 3.89, 2.18, and 2.60, respectively. The effects of pH and temperature on the retention of the fragmental and structural analogues were studied in detail. Van't Hoff analysis indicated that the retention and selectivity on FMIPs were an entropy-driven process, i.e., steric interaction. The resulting DMT-MIPs were used as a solid-phase extraction material to enrich CYR, MEL, TAT, and TME in different bio-matrix samples for high-performance liquid

chromatography analysis. The developed method had acceptable recoveries (86.8–98.6 %, $n=3$) and precision (2.7–4.6 %) at three spiked levels (0.05–0.5 $\mu\text{g g}^{-1}$).

Keywords Molecularly imprinted polymers · Multi-recognition · Fragmental template · Retention mechanism · Solid-phase extraction

Introduction

Molecularly imprinted polymers (MIPs) are materials based on the molecular-recognition properties derived from the polymerization of a mixture of functional monomers and cross-linking agent in the presence of a template. The synthetic cross-linked materials have cavities complementary to the size, shape, and functional groups of template molecules [1]. Because of distinctive features, including high selectivity, strong affinity, physical and chemical stability, and low cost of production, MIPs have been used in a wide range of application, such as solid-phase extraction (SPE) [2], chiral separation [3], chemical catalysis [4], drug delivery system [5], and chemical sensing [6].

Usually, the imprinted sites in MIPs are located not only on the surface but also in the interior area of highly cross-linked polymer. In this case, some binding sites are hard to approach, even after exhaustive washing with a lot of eluting solvents. Dead sites left are not involved in molecular recognition [7]. As a result, the potential risk of template leakage when using MIPs should not be neglected, which has the negative effects in detecting trace compounds through MIP-SPE.

To resolve the problem of template leakage, various strategies have been proposed, including isotope labeled imprinting [8], surface imprinting [9], semi-covalent imprinting [10], parallel MIP-SPE on blank samples [11], post-polymerization

Electronic supplementary material The online version of this article (doi:10.1007/s00216-015-8878-9) contains supplementary material, which is available to authorized users.

✉ Zhao-Sheng Liu
zhaoshengliu@sohu.com

¹ Tianjin Key Laboratory on Technologies Enabling Development of Clinical Therapeutics and Diagnostics (Theranostics), School of Pharmacy, Tianjin Medical University, 22 Qixiangtai Road, Heping District, Tianjin 300070, China

treatments [12], and approaches using pseudo-templates, which use analogues of target molecules as templates [13, 14]. As a result, even if the leakage of the “pseudo-template” happens in the process, the accuracy of the final result will not be affected. As for structures of dummy molecule, interval immobilization and fragment imprinting are two basic types. The former utilizes the compound with similar distance between two functional groups to target molecule as a pseudo-template to prepare MIPs [13]. However, it is difficult to find a suitable interval immobilization template since the two functional groups selected have to be limited to amino and carboxyl group. When the targets are expensive, highly toxic, unstable, and insoluble molecules, fragment imprinting, which uses a part of the target molecule as the pseudo-template [14], is especially valuable for the synthesis of MIPs since the fragmental template is easy to obtain from an existing chemical product library [1].

Previous research focused on the design and synthesis of the fragment molecularly imprinted polymers (FMIPs) which could effectively separate and enrich a single or a class of compounds. For example, MIPs for polychlorinated biphenyls were prepared by effective fragment potential molecular modeling approaches [14]. Clenbuterol and clorprenaline were also extracted from urine by imprinted microspheres which were synthesized using phenylephrine as fragmental template [15]. Molecularly imprinted monolith with melamine as fragmental template was prepared for selectively recognizing triamterene in human urine and serum [16].

Recently, in order to recognize more than one analyte simultaneously, several mixed-template imprinted polymer materials have been reported. Serotonin and histamine imprinted monolithic columns were used for evaluation of these templates in CEC [17]. Tetracycline antibiotics were extracted from food-stuff samples by imprinted microspheres using oxytetracycline and chlortetracycline as mixed template [18]. A hexachlorobenzene and 1,1,1-trichloro-2,2-bis(4-chlorophenyl) ethane imprinted biomimetic dendritic nanofiber-based piezoelectric sensor was developed for the determination of dichlorodiphenyltrichloroethane and hexachlorobenzene [19]. These mixed-template MIPs offer many advantages such as multi-recognition for different templates, low cost, and time saving. However, the potential risk of template leakage still exists.

Cyromazine (CYR, Fig. 1) is an insect growth regulator used for stock farming. It can be metabolized and form melamine (MEL, Fig. 1) in both plants and animals. The melamine can form insoluble complexes with cyanuric acid in the kidneys, so cyromazine and melamine always were simultaneously detected in food samples [20]. Triamterene (TAT, Fig. 1), banned for sport, is a potassium-sparing diuretic drug, which may pose serious health risks by secondary effects. So it is important to monitor the concentration of TAT in patients and sports [21]. Trimethoprim (TME, Fig. 1) is a broad spectrum

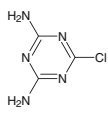
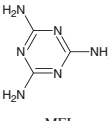
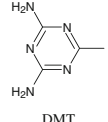
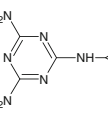
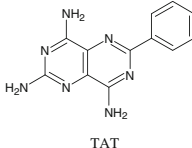
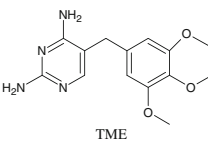
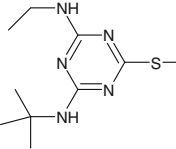
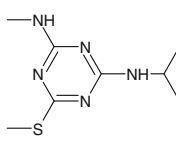
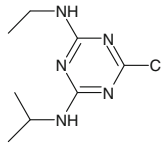
| | log P_{ow} | pK _a (pK _{a1}) | Molecular volume (cm ³ mol ⁻¹) |
|---|--------------|-------------------------------------|---|
|  CDT | -1.05 | No report | 107.69 |
|  MEL | -1.14 | 8.0 | 105.44 |
|  DMT | -0.39 | 4.6 | 110.71 |
|  CYR | 1.00 | 5.2 | 146.14 |
|  TAT | 0.98 | 6.2 | 216.68 |
|  TME | 0.91 | 7.2 | 263.16 |
|  TER | 3.48 | 4.2 | 230.62 |
|  DES | 2.38 | No report | 97.58 |
|  PRO | 2.89 | 1.9 | 193.23 |

Fig. 1 Chemical structures, log P_{ow} , pK_a, and molecular volume of 2,4-diamino-6-methyl-1,3,5-triazine (DMT), 2,4-diamino-6-chloro-1,3,5-triazine (CDT), melamine (MEL), cyromazine (CYR), triamterene (TAT), trimethoprim (TME), terbumeton (TER), desmetryn (DES), and propazine (PRO). log P_{ow} (octanol-water partition coefficient) was obtained by using Scifinder and calculated using ACDLabs Freeware (<http://www.acdlabs.com/home/>); pK_a was obtained by using Scifinder; molecular volume were calculated from software of Molinspiration (<http://www.molinspiration.com/>)

antibiotic, which is often combined with sulfonamides for achieving a synergetic antibacterial effect [22]. The relative pseudo-template MIPs for TME, TAT, CYR, and MEL have been prepared and applied [16, 20, 22]. These compounds all have the same fragment 2,4-diamino pyrimidinyl. If MIPs was prepared by pseudo-template including 2,4-diamino pyrimidinyl, it may simultaneously recognize TME, TAT, CYR, and MEL. But it is not published till now.

In this work, different FMIPs were prepared with 2,4-diamino-6-methyl-1,3,5-triazine (DMT), CYR, and TME as template, respectively, using methacrylic acid as functional monomer and ethylene glycol dimethacrylate as cross-linker. In contrast to the traditional MIPs synthesized using weak polar or non-polar organic solvents such as porogen [23, 24], polar ternary porogens composed of ionic liquid, methanol, and water were used to prepare the MIPs monolith. A detailed comparative analysis of their recognition properties was compared with an aim to check the recognition capability for CYR, MEL, TAT, and TME. Finally, the DMT-MIPs were used in MIPs solid-phase extraction (MISPE) protocols for selective extraction TAT, TME, CYR, and MEL from different bio-matrix samples, respectively.

Experimental

Reagents and standards

2,4-Diamino-6-methyl-1,3,5-triazine (DMT), cyromazine (CYR), melamine (MEL), triamterene (TAT), trimethoprim (TME), 2,4-diamino-6-chloro-1,3,5-triazine (CDT), terbumeton (TER), desmetyrn (DES), and propazine (PRO) were purchased from Sigma-Aldrich (St. Louis, MO, USA). Their chemical structures are shown in Fig. 1. Ethylene glycol dimethacrylate (EDMA) was from Tokyo Chemical Industry Co. Ltd. (Tokyo, Japan). Methacrylic acid (MAA), methanol (MeOH, HPLC grade), acetic acid, and 2,2'-azobisisobutyronitrile (AIBN) were purchased from Kermel Chemical Reagents Development Center (Tianjin, China). 1-Butyl-3-methylimidazolium tetrafluoroborate ([BMIM]BF₄) was from Shanghai Chengjie Reagent (Shanghai, China). Acetonitrile (MeCN, HPLC grade) was from Tianjin Biaoshiqi Chemical Reagent (Tianjin, China). All other reagents were analytical or HPLC grade from Tianjin Chemical Reagent Ltd. Co. (Tianjin, China).

The stock solutions were prepared by dissolving 50 mg of the substance (DMT or MEL or CYR or TAT or TME or CDT or TER or DES or PRO) in 100 mL of MeOH/water (1:1, v/v) and stored in the dark at 4 °C, respectively. To dissolve TAT and CDT, 5 mL dimethyl sulfoxide was added. The working solutions were prepared by direct dilution of the stock solution with MeOH immediately before use.

Preparation of FMIPs

To prepare FMIPs, a pre-polymerization solution was made with a mixture of 0.2 mmol template (DMT or CYR or TME), 1.6 mmol MAA, 6.0 mmol EDMA, 400 μ L MeOH, 100 μ L water, 2.0 mL [BMIM]BF₄, and 15 mg AIBN. Then the pre-polymerization mixture was introduced to the stainless steel tube (100 \times 4.6 mm i.d.). The tube was sealed and placed in a 60 °C water bath for 18 h. Then the column was connected to an HPLC pump and washed with MeCN, acetic acid/MeOH (1:9, v/v), and MeOH successively to remove porogen, template, and unreacted monomer and cross-linker. A blank column without imprinted molecule (NIPs) was synthesized in the same manner as the control.

Characterization

The morphology and size of the three FMIPs and NIPs were observed using a scanning electron microscopy (SEM; Hitachi X-650, Tokyo, Japan). Brunauer–Emmett–Teller (BET) surface areas and porosity of the FMIPs were measured on a V-Sorb 2800TP surface area and pore size analyzer (Gold APP Instruments, Beijing, China) at 77 K by nitrogen adsorption–desorption isotherms. Samples were vacuum degassed (10⁻³ Torr) at 60 °C for 4 h before the adsorption experiments.

Chromatographic evaluation

Chromatographic evaluation was carried out on the CoM 6000 HPLC system (CoMetro Technology, South Plainfield, NJ, USA) including a 6000 LDI pump, a Rheodyne 7725 injector with a 20 μ L loop, a Co-IV column temperature controller, and a 6000 UV–vis detector. Data processing was performed with an EZChrom workstation. Detection wavelength was 214 nm for MEL and CYR, 367 nm for TAT, and 280 nm for TME, and column temperature was set at 30 °C. Mobile phase was pumped through the column at a flow rate of 1 mL min⁻¹. All of the mobile phases were filtered through a 0.22- μ m membrane filter (Millipore) prior to use. The capacity factor (*k*) for analyte was calculated as $(t_R - t_0)/t_0$, where *t_R* is the retention time of the analyte and *t₀* is the retention time of unretained acetone. The imprinting factor (IF) was calculated as $IF = k_{MIP}/k_{NIP}$, where *k_{MIP}* and *k_{NIP}* are the *k* of analyte on MIPs and NIPs column, respectively. The selectivity factor (α) was calculated as $\alpha = k_1/k_2$, where *k₁* and *k₂* are the *k* of imprinting template and analogue, respectively.

MISPE and determination of MEL, CYR, TAT, and TME in different samples

The solid-phase extraction cartridges (3 mL) were packed with 200 mg of DMT-MIPs. Prior to each extraction, the cartridges were consecutively equilibrated with 3.0 mL of MeOH

and 3.0 mL of water. Milk and egg samples were obtained from the market near Tianjin Medical University (Tianjin, China), and human serum samples were collected from a drug-free healthy volunteer in our department. All samples were stored at $-20\text{ }^{\circ}\text{C}$ until the assay. Then 20 μL of the standard working solution and 3.0 mL MeCN solution were added to 1.0-mL samples (MEL and CYR in milk, TAT in human serum, and TME in egg, respectively). The samples were vortex-mixed for 1 min and centrifuged at 10,000 rpm for 10 min. The supernatant was loaded onto cartridges, then 2 mL of MeCN was percolated through for washing matrix interference. The analytes were eluted with 5 mL MeOH-ammonia (95:5, *v/v*). The elution fractions were collected and dried under a nitrogen stream. The residue was dissolved in 200 μL mobile phase for further HPLC analysis.

Chromatographic separation of TAT, MEL, and CYR was performed on a BaseLine SCX column (150 \times 4.6 mm, I.D., 4 μm) from Tianjin BaseLine Chromtech Research Centre (Tianjin, China). For MEL and CYR, the mobile phase was MeOH-water (50 mM KH_2PO_4 , pH 3.0) (30:70, *v/v*), and detection wavelength was set as 214 nm. For TAT, the mobile phase was MeOH-water (20 mM NaAc, pH 4.0) (60:40, *v/v*), and detection wavelength was 367 nm. Quantitative analysis of TME was performed on an Aqua C18 column (250 \times 4.6 mm, I.D., 5 μm) from Phenomenex (Torrance, USA). The mobile phase was MeCN-water-triethylamine (adjusted to pH 6.4 by NaOH) (200:799:1, *v/v/v*), and detection wavelength was 280 nm. The flow rates of mobile phase were maintained at 1.0 mL min^{-1} , and the injection volume was 20 μL .

Results and discussion

Preparation and characterization of FMIPs

The preparation of MIPs from conventional bulk polymerization has to be grounded and sieved to appropriate size. In addition, some of the imprinted sites may be destroyed in this time-consuming process. Monolithic MIPs prepared by in situ polymerization is one of the promising approaches to overcome the problems mentioned previously; therefore, FMIPs are synthesized in monolithic format. Previous studies have demonstrated that an appropriate porogenic solvent is a critical factor to achieve MIPs with highly selective recognition properties [25, 26]. In most cases, template and monomers can interact through hydrogen bonding, thus aprotic and weakly polar solvents are selected to promote the formation of imprinting complex. In the present study, all of the fragmental templates containing 2,4-diamino pyrimidinyl were insoluble in non-polar solvent. A series of various porogenic solvent mixtures, including MeOH, water, tetrahydrofuran, dimethyl formamide, and dimethyl sulfoxide, were attempted to solve

the problem. It was found that the polar porogenic mixture of MeOH and water can yield good selectivity, but leads to the MIPs monolith with low permeability. When the solvent mixture containing ionic liquid was used as porogen, MIPs monolith with lower back pressure and higher selectivity can be achieved [27]. Given the facts previously mentioned, a new ternary porogen composed of ionic liquid ([BMIM]BF₄), MeOH, and water was developed to prepare FMIPs. In our study, MAA was found to be the optimum functional monomer in terms of IF. EDMA was chosen as cross-linker due to good solubility in the ternary porogen. DMT, CYR, and TME were chosen as templates to prepare DMT-MIPs, CYR-MIPs, and TME-MIPs, respectively.

SEM is an appropriate method used for observing the structures of a polymer. As shown in Fig. 2, the internal textures of the FMIPs monolith present that microglobules of relative size were agglomerated to larger clusters. The size of microglobules of different FMIPs increased with decreasing molecular volume of the template (Fig. 1). When TME was the template, the size was 2–4 μm , whereas when DMT was the template, the size was 4–6 μm . This result indicates that template had a prominent impact on the morphology of FMIPs.

The data of BET surface area and pore volume of the FMIPs are given in Table 1. The NIPs had a larger surface area than the other three FMIPs. This indicated that the specific selectivity of FMIPs was irrelevant to the surface area, but about the imprinting sites. Larger specific pore volume and average pore width were also observed on the NIPs. This discrepancy may be due to the presence of different fragmental templates. In contrast to previous reports [28], in this context, the template effect on the pore structure of the resulting FMIPs was little. Thus, the contribution of pore structure to the imprinting effect of the FMIPs was minor compared with the interaction between functional monomer and the template.

Selectivity of FMIPs

To evaluate the selectivity of three FMIPs, IFs of the fragmental template and analogues were investigated using MeCN-water (70:30, *v/v*) as mobile phase. As shown in Fig. 1, CDT, DMT, MEL, CYR, TAT, and TME were fragmental analogues containing 2,4-diamino pyrimidinyl group, while TER, DES, and PRO were structural analogues containing a triazine ring. The FMIPs only could recognize the former, but not the latter. From the IF value (Fig. 3), it can be seen clearly that the FMIPs possessed the best specific recognition ability to the relative template. The greatest IF was 5.25, 6.69, and 7.11 of DMT on DMT-MIPs, CYR on CYR-MIPs, and TME on TME-MIPs, respectively.

From a comparison of the IF value of the fragmental analogues, it was indicated that the selectivity of the FMIPs to fragmental analogue was associated with the molecular

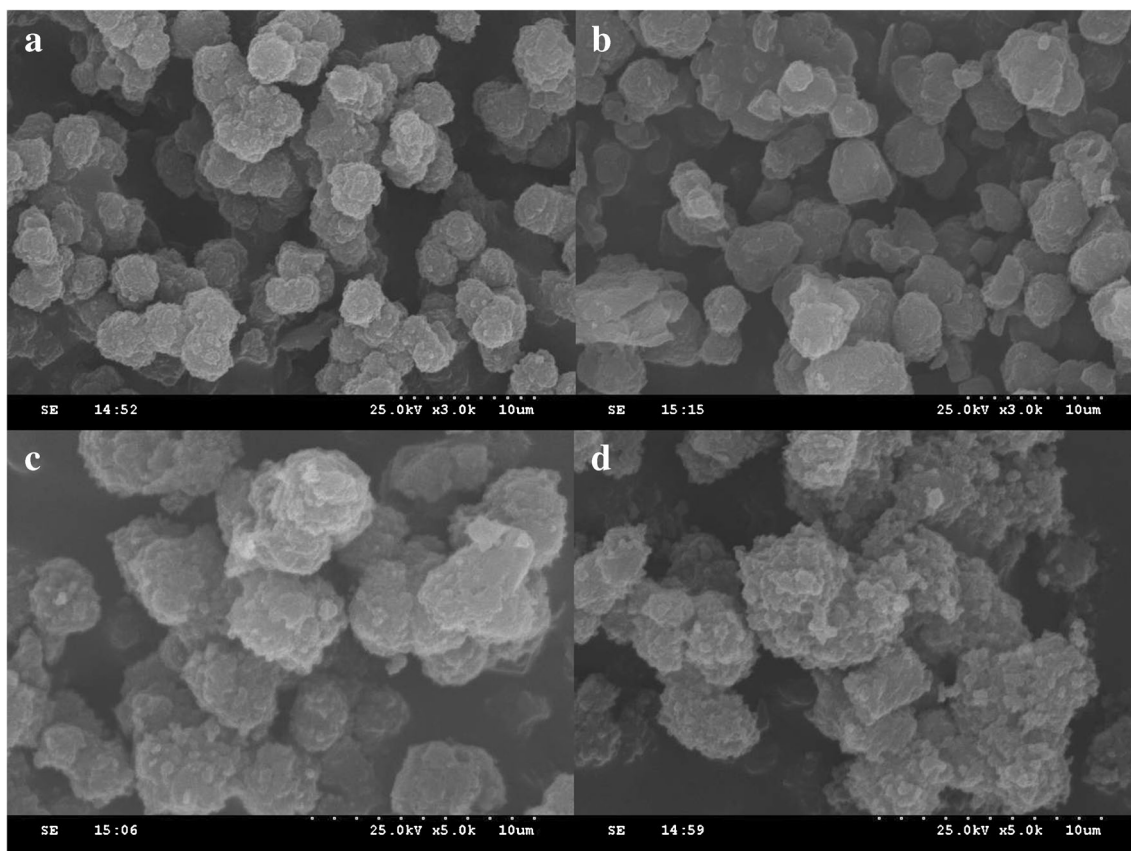


Fig. 2 SEM of the TME-MIPs (a), CYR-MIPs (b), DMT-MIPs (c), and NIPs (d)

volume of analogue and template (Fig. 1). The magnitude order of molecular volume was TME>TAT>CYR>DMT>CDT>MEL. On DMT-MIPs, the IF of the fragmental analogue decreased with increasing molecular volume. Conversely, the IF increased with increasing molecular volume on TME-MIPs. The exception to the rule was MEL, which could retain much longer due to the structure of 2,4-diamino pyrimidinyl in the template. These results suggested that the affinity of FMIPs to the fragmental analogue increased with the increase in the similarity of their molecular volume to the template. An increasing trend can be observed on the CYR-MIPs. In addition, for TME-MIPs, very low IF of DMT (1.52) and CDT (1.07) suggested that the larger template molecule

(the molecular volume of $263.16 \text{ cm}^3 \text{ mol}^{-1}$ for TME) is inappropriate for preparing MIPs to recognize small molecule (the molecular volumes of $107.69 \text{ cm}^3 \text{ mol}^{-1}$ for CDT and $110.71 \text{ cm}^3 \text{ mol}^{-1}$ for DMT). When the molecular volume of the target molecule is less than one half of the template molecule, the specific recognition is lost. These results imply

Table 1 Summary of the BET surface area and the pore data for FMIPs and NIPs

| Polymers | DMT-MIPs | CYR-MIPs | TME-MIPs | NIPs |
|---|----------|----------|----------|--------|
| $S_{\text{BET}} (\text{m}^2 \text{ g}^{-1})^{\text{a}}$ | 286.75 | 263.22 | 281.53 | 307.72 |
| $V_{\text{p}} (\text{cm}^3 \text{ g}^{-1})^{\text{b}}$ | 0.344 | 0.305 | 0.348 | 0.423 |
| $D_{\text{p}} (\text{nm})^{\text{c}}$ | 4.79 | 4.64 | 4.95 | 5.50 |

^a BET surface area

^b Single point adsorption total pore volume

^c Total adsorption average pore width

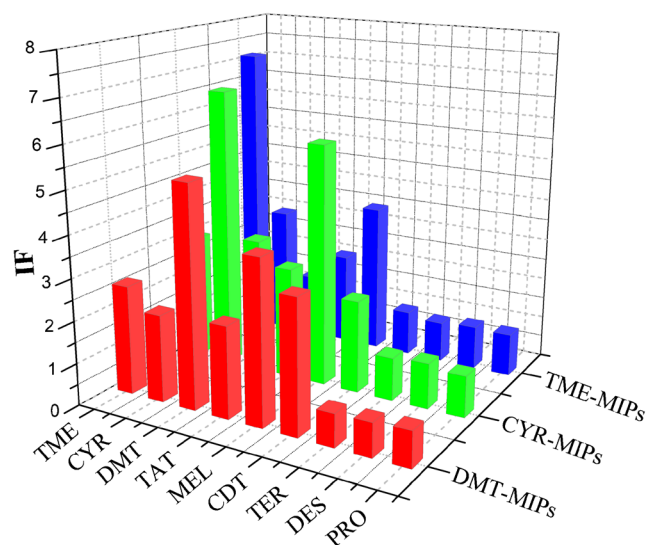


Fig. 3 IFs of analytes on different FMIPs

that the desired template in fragment imprinting should be those where the molecular volume is not smaller than half of the used template in addition to the same fragment (or same group) of target molecule or structure analogue.

Effect of organic modifier

The influence of organic modifier on k of fragmental template and analogue was carried out on different FMIPs. A mixture of MeCN-water was used as mobile phase, with MeCN content from 62.5 to 77.5 %. As shown in Fig. S1 in the Electronic Supplementary Material (ESM), the template and fragmental analogues had a similar trend of increase in k with increasing MeCN content in the mobile phase. This may be due to the presence of imprinted sites containing 2,4-diamino pyrimidinyl moiety. In contrast to water, MeCN as mobile phase could improve the stability of hydrogen bond between carboxyl and amino groups, resulting in the increased retention of the fragmental analogues on FMIPs [29]. However, structural analogues had displayed different retention properties in that k decreased with the increase in MeCN content, a typical reversed-phase behavior [30]. In addition, when using MAA as functional monomer, the strength of monomer-template interaction is strongly influenced by basicity of the template [29]. This means that the more basic templates will lead to the more strong interaction with monomers, which promotes a large number of imprinting sites with optimal arrangement of carboxylic acid groups to bind with the 2,4-diamino pyrimidinyl group. In Fig. 4, a notable increase in affinity and selectivity with increasing pK_a of the template occurs. The low k showed the presence of non-specific binding (hydrophobic interaction) on the NIPs. These results indicated that for the template and fragmental analogues, a mixed-mode retention mechanism on FMIPs may be present: one is the interaction between the imprinted cavity and template or

fragmental analogues, and the other is hydrophobic interaction derived from hydrophobic polymer skeleton. On the contrary, the structural analogues of the template were retained only by hydrophobic interaction.

Effect of pH

The influence of pH on retention behaviors of template and analogues was studied by using MeCN/sodium acetate buffer (50 mM) (70:30, v/v) as mobile phase. The pH was adjusted by changing the ratio of acetic acid to sodium acetate solution. The k of the template and analogues on different FMIPs are shown in Fig. S2 in the ESM. Compared with ESM Fig. S1, by using the same organic-aqueous mobile phase with sodium acetate added, a clear dependence of k on the buffer salts was seen with weaker retention and lower selectivity. The result suggested that the retention could be modulated by controlling buffer salts of mobile phase. In addition, the maximum k of all fragmental analogues on three FMIPs was observed at pH 4.6. Considering that the pK_a of MAA is 4.66, this finding may be attributed to the suppressed ionization of carboxyl groups from the imprinted cavity in polymer skeleton, which is beneficial to the ionic interaction between the groups with amino groups of template and fragmental analogues. When the pH of the mobile phase was higher than the pK_a value of the template, the retention decreased because of the deprotonation of carboxyl groups. Similarly, at lower pH, the ionization of carboxyl groups was suppressed, but the vast majority of amino groups were ionized, thus the retention of template and fragmental analogues on the imprinted monoliths also decreased. Previous studies have shown that the template retention and selectivity on the MIPs based on MAA-EDMA system followed a simple ion-exchange model [29], and the maximum retention of template was observed at pH close to pK_a of template [31]. In contrast, the maximum retention of the template and fragmental analogues on FMIPs was observed at the pK_a of MAA.

It was found that the magnitude order of k on DMT-MIPs was MEL, CYR, TAT, DMT, TME, and CDT. Corresponding order on CYR-MIPs was CYR, MEL, TAT, TME, DMT, and CDT. In contrast, for TME-MIPs, the order was TME, TAT, CYR, MEL, and DMT. The results were inconsistent with the rank of IFs for the relative FMIPs. This suggested a mixed mode of retention mechanism as discussed in “Effect of organic modifier” section. On DMT-MIPs, IF of CDT was 3.18 and higher than that of CYR (2.08), TAT (2.18), and TME (2.60), but CDT was the first one to be washed out at pH 4.6. On the control polymer, the lower IF value of CYR than other fragmental analogues was observed (Fig. 3). This may be the result of hydrophobic interaction between cyclopropyl on CYR and polymer skeleton, leading to the greatest k . To investigate the effect of different hydrophobicities of templates, three kinds of FMIPs were prepared with relative-

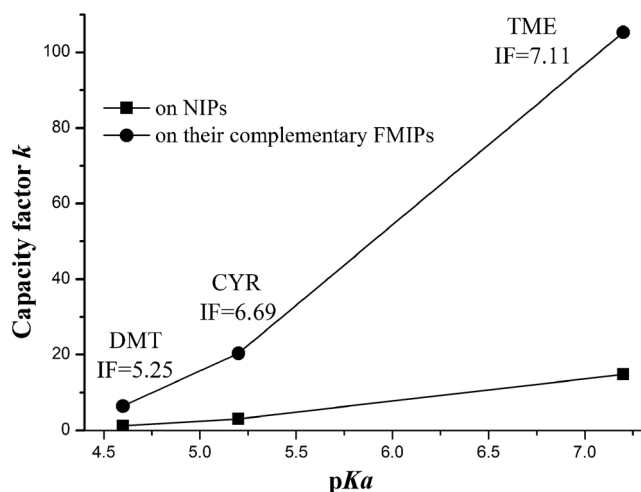


Fig. 4 k versus pK_a of DMT, CYR, and TME on their complementary FMIPs as well as on NIPs

hydrophobic CYR ($\log P_{ow}=1.00$), medium-hydrophobic TME ($\log P_{ow}=0.91$), and less-hydrophobic DMT ($\log P_{ow}=-0.39$), respectively. As shown in Fig. 5, the retention of templates on FMIPs with complementary sites increased with increasing $\log P_{ow}$ values, which was similar to the retention mechanism of reversed phase chromatography [29], suggesting the mixed-mode retention mechanism.

Stoichiometric displacement model for retention

In stoichiometric displacement model for retention (SDM-R) model, the simulation of chromatographic data was carried out using the following equation [32]:

$$\ln k = \ln A - Z[I] \quad (1)$$

where k is for the capacity factor and $[I]$ is the solvent activity in bulk solution. When other conditions remain unchanged, water added in the mobile phase is viewed as the displacer and $[I]$ is the water percentage in the mobile phase. $\log A$ is the affinity of analyte to imprinted stationary phase. Z represents the total number of solvent molecule released from the binding sites on FMIPs, together with its corresponding contact area between analyte and FMIPs.

Figures of $\ln k$ versus $[I]$ about three FMIPs are shown in Fig. 6. The numerical values of $\ln A$, Z , and R^2 are calculated and summarized in Table 2. The good linear relationship between k of each analyte and changes of water percentage demonstrated that the retention behavior of all analytes on three FMIPs could be successfully fitted with SDM-R. Equilibrium, which existed between imprinted stationary phase and displacer with a certain concentration, was broken when separated analytes entered into imprinted sites and were adsorbed by imprinted stationary phase. In addition, since water was

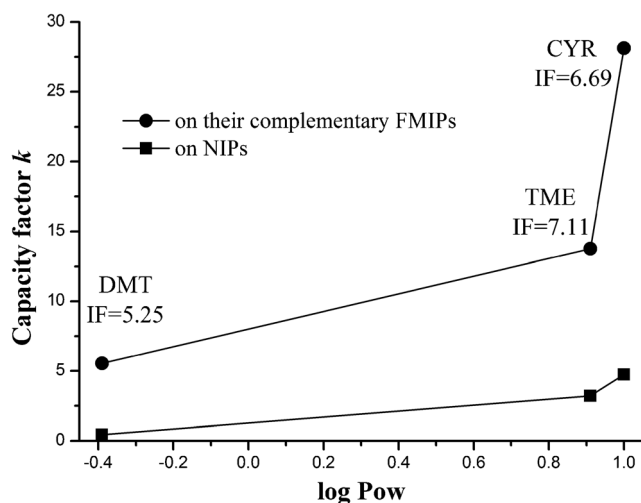


Fig. 5 k versus $\log P_{ow}$ of DMT, CYR, and TME on their complementary FMIPs as well as on NIPs

used as strong displacer, the increased water content in the mobile phase should lead to a decrease in the retention of analyte on FMIPs. However, the retention order of structure analogues on three FMIPs and CDT on TME-MIPs reversed when MeCN was used a displacer for their separation.

Second, on the same FMIPs, the rank of $\ln A$ for template and analogues agreed very well with the order of k reported, suggesting that $\ln A$ could be used to evaluate the retention characteristics of FMIPs. On different FMIPs, the $\ln A$ value of template was greater than its analogues.

There was no obvious regularity on the value of Z . One possible reason was that different fragmental analogues could be adsorbed by different sites on the FMIPs, including imprinted and hydrophobic site, as confirmed in “Effect of organic modifier” and “Effect of pH” sections. In addition, imprinted sites are heterogeneous, which results from excess monomer [33] and non-well-defined pre-polymerization step [34]. As a consequence, at least three kinds of action sites on FMIPs were responsible for the different adsorption ability to the fragmental analogues.

Van't Hoff analysis

To investigate the nature of interactions involved in separation processes, the temperature effect on both the k and selectivity factor of the fragmental and structural analogues was carried out at different temperatures (25–45 °C). As column temperature increased, the retention of analogues on fragment imprinted monolith substantially decreased, indicating that the separation for these analogues was exothermic [35].

The temperature dependence of k and selectivity factor can be processed by the Van't Hoff equation [36].

$$\ln k = -\frac{\Delta H}{RT} + \frac{\Delta S}{R} + \ln \varphi \quad (2)$$

$$\ln a = -\frac{\Delta \Delta H}{RT} + \frac{\Delta \Delta S}{R} \quad (3)$$

R and φ are the gas constant and the phase volume ratio, respectively. The Van't Hoff plots for separation of fragmental and structural analogues showed good linearity (see ESM Fig. S3), indicating no changes in retention mechanisms of analytes within the temperature range studied. According to Eq. 2, the thermodynamic terms, $-\Delta H/RT$ and $\Delta S/R + \ln \varphi$, were calculated at 313 K and listed in Table 3. The values of $\Delta \Delta H$ and $\Delta \Delta S$ calculated from the intercepts and the slopes of Eq. 3 are also summarized in Table 3.

The results showed that (1) in general, the transfer of fragmental analogues from mobile phase to imprinted stationary phase was controlled by positive ΔH and ΔS ; (2) the selective separation of fragmental analogues on different FMIPs was an entropy-controlled process because $|\Delta S/R + \ln \varphi| > |-\Delta H/RT|$ and $|T \Delta \Delta S| > |\Delta \Delta H|$ [37]; (3) the magnitude order of

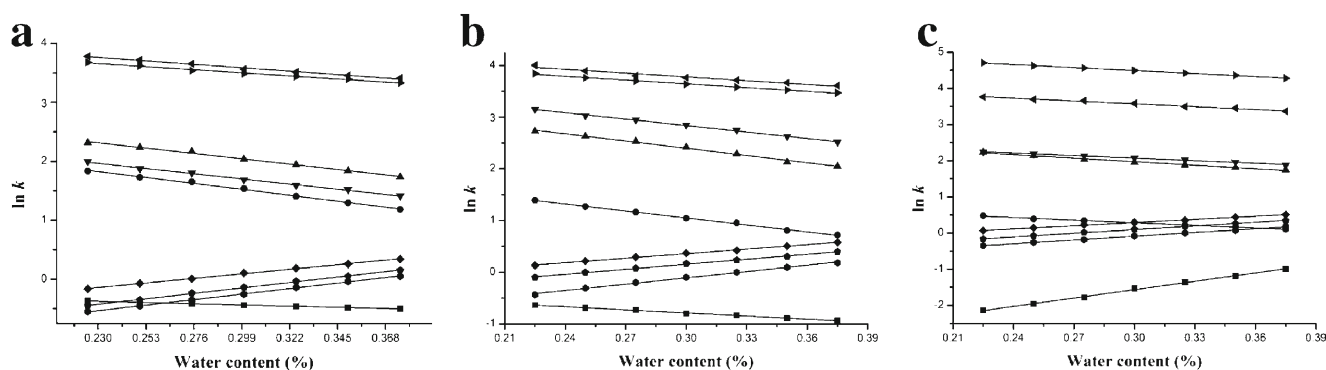


Fig. 6 Plots of $\ln k$ vs. $[I]$ on DMT-MIPs (a), CYR-MIPs (b), and TME-MIPs (c). ■ CDT, ● DMT, ▲ MEL, ▼ CYR, ◀ TAT, ▶ TME, ◆ TER, ◆ DES, ◆ PRO. HPLC conditions: column temperature, 30 °C; mobile

phase, MeCN with 22.5–37.5 % water (v/v); detection, 214 nm for MEL and CYR, 367 nm for TAT, 280 nm for TME; flow rate, 1.0 mL min⁻¹

entropic term ($\Delta S/R + \ln \varphi$) for fragmental analogues in FMIPs was consistent with the order of chromatographic peaks eluted; and (4) the template had larger values of entropic term than its fragmental analogues. For example, the values of entropic term for CYR on CYR-MIPs, DMT-MIPs, and TME-MIPs were 3.01, 2.31, and 2.35, respectively.

In this case, with larger intercept and lower slope in Van't Hoff equation, a contribution of entropic term should be much evident, while the temperature dependence of enthalpic term should be less pronounced. In other words, if the FMIPs have imprinted cavity complementary to fragmental analogues, the steric interaction between FMIPs and fragmental analogues should play an important role. In all FMIPs, the smaller contribution of enthalpic term was compensated by the higher contribution of entropic term [38, 39]. The weighted entropic term implied strong steric interaction between fragmental analogues and imprinted sites of the FMIPs.

Previously, the retention mechanisms of a number of MIPs, which were depending on analytes and mobile phase, have been shown in ESM Table S1. For example, on the Fmoc-L-Trp-MIPs, the separation of Fmoc-L-Trp was entropy driven,

while the separation of structural analogues (L-enantiomers) was enthalpy driven [40, 41]. On the CD-MIPs, the stereo-separation process was entropy driven and enthalpy driven for the mobile phase of pH 4.2 and 11.7, respectively [42]. In this work, by using the MeCN-buffer salts as mobile phase, a strong retention of the fragmental analogues on FMIPs was observed. This meant that the steric interaction during the binding process between analyte and sites played a major role in the binding analogues to the surface of FMIPs.

Application of FMIPs for MISPE of MEL, CYR, TAT, and TME from different samples

HPLC-UV was used to determine MEL, CYR, TAT, and TME, and the analytical data are listed in ESM Table S2. The linear range was 200 to 2500 ng mL⁻¹, with R^2 of over 0.999. The LODs (signal/ratio, 3:1) range from 10 to 30 ng mL⁻¹, and the LOQs (signal/ratio, 10:1) range from 35 to 100 ng mL⁻¹.

To demonstrate the potential of FMIPs for the selective samples cleanup and to avoid template leakage, the DMT-

Table 2 SDM-R results of fragmental and structural analogues on different FMIPs

| Analytes | DMT-MIPs | | | CYR-MIPs | | | TME-MIPs | | |
|----------|----------|--------|-------|----------|--------|-------|----------|--------|-------|
| | $\ln A$ | Z | R^2 | $\ln A$ | Z | R^2 | $\ln A$ | Z | R^2 |
| CDT | -0.174 | 0.878 | 0.994 | -0.186 | 2.014 | 0.995 | -3.881 | -7.728 | 0.998 |
| DMT | 2.830 | 4.366 | 0.999 | 2.404 | 4.514 | 0.996 | 1.014 | 2.425 | 0.993 |
| MEL | 3.223 | 3.948 | 0.996 | 3.806 | 4.686 | 0.994 | 2.956 | 3.270 | 0.993 |
| CYR | 2.846 | 3.828 | 0.993 | 4.082 | 4.143 | 0.994 | 2.786 | 2.373 | 0.990 |
| TAT | 4.347 | 2.535 | 0.992 | 4.519 | 2.458 | 0.996 | 4.359 | 2.617 | 0.992 |
| TME | 4.186 | 2.288 | 0.993 | 4.378 | 2.437 | 0.998 | 5.329 | 2.783 | 0.998 |
| TER | -0.912 | -3.356 | 0.998 | -0.522 | -2.930 | 0.998 | -0.587 | -2.930 | 0.998 |
| DES | -1.347 | -4.011 | 0.999 | -0.812 | -3.217 | 0.997 | -0.921 | -3.392 | 0.998 |
| PRO | -1.470 | -4.072 | 0.999 | -1.332 | -4.073 | 0.997 | -1.128 | -3.469 | 0.998 |

Table 3 Thermodynamic parameters of separation for fragmental and structural analogues on different FMIPs

| Monoliths | Analytes | $-\Delta H/RT^a$ | $\Delta S/R+\ln\varphi^b$ | R^2 | $\Delta\Delta H^b$ | $\Delta\Delta S^b$ | R^2 |
|-----------|----------|------------------|---------------------------|-------|--------------------|--------------------|-------|
| DMT-MIPs | CDT | 0.17 | 0.33 | 0.996 | 0.08 | 16.61 | 0.872 |
| | DMT | 0.20 | 1.67 | 0.992 | – | – | – |
| | MEL | 0.29 | 1.87 | 0.991 | –0.60 | –5.35 | 0.989 |
| | CYR | 0.43 | 2.31 | 0.994 | –0.24 | –1.68 | 0.988 |
| | TAT | 0.09 | 3.64 | 0.997 | 0.30 | –16.41 | 0.991 |
| | TME | 0.09 | 3.55 | 0.995 | 0.29 | –15.67 | 0.988 |
| | TER | 0.09 | 0.19 | 0.993 | 0.28 | 12.28 | 0.967 |
| | DES | 0.12 | –0.03 | 0.998 | 0.20 | 14.11 | 0.948 |
| | PRO | 0.14 | –0.13 | 0.998 | 0.17 | 14.99 | 0.964 |
| CYR-MIPs | CDT | 0.21 | –0.68 | 0.997 | 0.34 | 12.05 | 0.974 |
| | DMT | 0.27 | 1.21 | 0.994 | 0.19 | 15.28 | 0.936 |
| | MEL | 0.20 | 2.55 | 0.993 | 0.36 | 4.18 | 0.971 |
| | CYR | 0.34 | 3.06 | 0.990 | – | – | – |
| | TAT | 0.37 | 3.99 | 0.994 | –0.09 | –7.75 | 0.932 |
| | TME | 0.35 | 3.85 | 0.993 | –0.04 | –6.64 | 0.886 |
| | TER | 0.01 | 0.41 | 0.999 | 0.68 | 21.93 | 0.983 |
| | DES | 0.12 | 0.24 | 0.995 | 0.57 | 23.42 | 0.979 |
| | PRO | 0.13 | –0.01 | 0.998 | 0.54 | 25.50 | 0.968 |
| TME-MIPs | CDT | 0.27 | –1.37 | 0.997 | 0.19 | –7069.21 | 0.914 |
| | DMT | 0.28 | 0.48 | 0.997 | 0.16 | 35.23 | 0.986 |
| | MEL | 0.46 | 2.25 | 0.997 | –0.30 | 20.52 | 0.992 |
| | CYR | 0.42 | 2.35 | 0.997 | –0.18 | 19.69 | 0.992 |
| | TAT | 0.08 | 3.63 | 0.996 | 0.70 | 9.02 | 0.996 |
| | TME | 0.35 | 4.72 | 0.997 | – | – | – |
| | TER | 0.12 | 0.37 | 0.994 | 0.59 | 36.15 | 0.990 |
| | DES | 0.13 | 0.19 | 0.997 | 0.55 | 37.65 | 0.986 |
| | PRO | 0.16 | 0.02 | 0.996 | 0.49 | 39.06 | 0.978 |

^a Calculated at $T=313$ K, $R=8.314$ J mol^{–1} K^{–1}, ΔH (kJ mol^{–1})

^b ΔS (J mol^{–1} K^{–1}), $\Delta\Delta H$ (kJ mol^{–1}), $\Delta\Delta S$ (J mol^{–1} K^{–1})

MIPs were employed in the purification of spiked MEL and CYR in milk, TAT in serum, and TME in egg samples, and the extracted fractions were analyzed by HPLC. The above samples spiked with different concentrations of analytes were detected, and the results are shown in Table 4. When the concentration increased

from 0.05 to 0.5 $\mu\text{g mL}^{-1}$, the mean recovery rate ranged from 89.6 to 98.6 % with relative standard deviations (RSD) less than 4.6 % for MEL and CYR, from 86.8 to 94.8 % with RSD less than 3.9 % for TAT, and from 90.5 to 96.4 % with RSD less than 3.5 % for TME. These results demonstrated that the

Table 4 Average recoveries of MEL, CYR, TAT, and TME from different spiked samples

| Sample | Analyte | Spiked | | | | | |
|--------|---------|----------------------------|---------|---------------------------|---------|---------------------------|---------|
| | | 0.05 $\mu\text{g mL}^{-1}$ | | 0.1 $\mu\text{g mL}^{-1}$ | | 0.5 $\mu\text{g mL}^{-1}$ | |
| | | Recovery (%) | RSD (%) | Recovery (%) | RSD (%) | Recovery (%) | RSD (%) |
| Milk | MEL | 91.5 | 3.6 | 95.3 | 2.7 | 98.6 | 4.6 |
| | CYR | 89.6 | 4.2 | 93.4 | 3.8 | 97.2 | 4.2 |
| Serum | TAT | 86.8 | 3.6 | 89.1 | 3.9 | 94.8 | 3.8 |
| Egg | TME | 90.5 | 2.9 | 93.5 | 3.5 | 96.4 | 2.8 |

MISPE combined with HPLC analysis can be used for the determination of MEL, CYE, TAT, and TME in bio-matrix samples.

Conclusion

The FMIPs were successfully prepared in a polar ternary porogen, [BMIM]BF₄, MeOH, and water. By investigating the retention properties of the template analogues on different FMIPs, a rational principle of choosing fragmental template was suggested that desired fragmental template should have the molecular volume of target molecule not less than one half of the template molecule in addition to a similar (or smaller) molecular structure of the target molecule, including the same fragment (or the same group on similar structure). Furthermore, the *k* of fragmental analogues on FMIPs were inconsistent with the rank of their IFs, indicating the presence of mixed-mode retention mechanisms for fragmental analogues, i.e., imprinting effect and hydrophobic interaction. In the process of investigating the effects of water ratio in mobile phase on retention of fragmental analogues, chromatographic data could be successfully fitted with SDM-R. Additionally, the results of Van't Hoff analysis indicated that the separation of fragmental analogues on FMIPs was an entropy-controlled process, and steric interaction was the major retention mechanism. The successful application MISPE-HPLC method suggests that FMIPs could be a promising alternative for multi-recognition extraction of MEL, CYE, TAT, and TME in complex bio-matrix samples.

Acknowledgments This work was supported by the National Natural Science Foundation of China (Grant No. 21375096 and U1303202) and by the Hundred Talents Program of the Chinese Academy of Sciences.

References

- Chen LX, Xu SF, Li JH (2011) Recent advances in molecular imprinting technology: current status, challenges and highlighted applications. *Chem Soc Rev* 40(5):2922–2942
- Toth B, Horvai G (2012) Chromatography, solid-phase extraction, and capillary electrochromatography with MIPs. *Top Curr Chem* 325:267–306
- Kulsing C, Knob R, Macka M, Junor P, Boysen RI, Hearn MTW (2014) Molecularly imprinted polymeric porous layers in open tubular capillaries for chiral separations. *J Chromatogr A* 1354(8):85–91
- Orozco J, Cortes A, Cheng G, Sattayasamisathit S, Gao W, Feng XM, Shen YF, Wang J (2013) Molecularly imprinted polymer-based catalytic micromotors for selective protein transport. *J Am Chem Soc* 135(14):5536–5539
- Li B, Xu JJ, Hall AJ, Haupt K, Bui BTS (2014) Water-compatible silica sol-gel molecularly imprinted polymer as a potential delivery system for the controlled release of salicylic acid. *J Mol Recognit* 27(9):559–565
- Fuchs Y, Soppera O, Mayes AG, Haupt K (2013) Holographic molecularly imprinted polymers for label-free chemical sensing. *Adv Mater* 25(4):566–570
- Chen FF, Xie XY, Shi YP (2013) Preparation of magnetic molecularly imprinted polymer for selective recognition of resveratrol in wine. *J Chromatogr A* 1300(26):112–118
- Kawaguchi M, Hayatsu Y, Nakata H, Ishii Y, Ito R, Saito K, Nakazawa H (2005) Molecularly imprinted solid phase extraction using stable isotope labeled compounds as template and liquid chromatography-mass spectrometry for trace analysis of bisphenol A in water sample. *Anal Chim Acta* 539(1–2):83–89
- Bognar J, Szucs J, Dorko Z, Horvath V, Gyurcsanyi RE (2013) Nanosphere lithography as a versatile method to generate surface-imprinted polymer films for selective protein recognition. *Adv Funct Mater* 23(37):4703–4709
- Cacho C, Turiel E, Martin-Esteban A, Ayala D, Perez-Conde C (2006) Semi-covalent imprinted polymer using propazine methacrylate as template molecule for the clean-up of triazines in soil and vegetable samples. *J Chromatogr A* 1114(2):255–262
- Berffren C, Bayouth S, Sherrington D, Ensing K (2000) Use of molecularly imprinted solid-phase extraction for the selective clean-up of clenbuterol from calf urine. *J Chromatogr A* 889(1–2):105–110
- Ellwanger A, Berggren C, Bayouth S, Crencenzi C, Karlsson L, Owens PK, Ensing K, Cormack P, Sherrington D, Sellergren B (2001) Evaluation of methods aimed at complete removal of template from molecularly imprinted polymers. *Analyst* 126(6):784–792
- Kubo T, Kuroda K, Tominaga Y, Naito T, Sueyoshi K, Hosoya K, Otsuka K (2014) Effective determination of a pharmaceutical, sulphiride, in river water by online SPE-LC-MS using a molecularly imprinted polymer as a preconcentration medium. *J Pharm Biomed* 89(15):111–117
- Cleand D, McCluskey A (2013) The use of effective fragment potentials in the design and synthesis of molecularly imprinted polymers for the group recognition of PCBs. *Org Biomol Chem* 11(28):4646–4656
- Yan HY, Liu ST, Gao MM, Sun N (2013) Ionic liquids modified dummy molecularly imprinted microspheres as solid phase extraction materials for determination of clenbuterol and clorprenaline in urine. *J Chromatogr A* 1294(14):10–16
- Zhao XY, Zhang HW, Liang ZJ, Shu YP, Liang Y (2013) Selective recognition of triamterene in biological samples by molecularly imprinted monolithic column with a pseudo template employed. *J Sep Sci* 36(9–10):1501–1508
- Zaidi SA (2013) Dual-templates molecularly imprinted monolithic for the evaluation of serotonin and histamine in CEC. *Electrophoresis* 34(9–10):1375–1382
- Jing T, Wang Y, Dai Q, Xia H, Niu JW, Hao QL, Mei SR, Zhou YK (2010) Preparation of mixed-templates molecularly imprinted polymers and investigation of the recognition ability for tetracycline antibiotics. *Biosens Bioelectron* 25(10):2218–2224
- Prasad BB, Jauhari D (2015) A dual-template biomimetic molecularly imprinted dendrimer-based piezoelectric sensor for ultratrace analysis of organochlorine pesticides. *Sensor Actuators B Chem* 207(Part A):542–551
- Wang XH, Fang QX, Liu SP, Chen L (2012) Preparation of a magnetic molecularly imprinted polymer with pseudo template for rapid simultaneous determination of cyromazine and melamine in bio-matrix samples. *Anal Bioanal Chem* 404(5):1555–1564
- Nezhadali A, Mojarrab M (2015) Fabrication of an electrochemical molecularly imprinted polymer triamterene sensor based on multivariate optimization using multi-walled carbon nanotubes. *J Electroanal Chem* 744(1):85–94

22. Zhang HW, Guo JW, Li K, Wang WS, Wu YP, Lu QW, Zhai HY (2012) On-line determination of trimethoprim in human serum by molecularly imprinted monolithic column with melamine employed as analogue template. *Chin J Anal Chem* 40(5):699–704
23. Quaglis M, Chenon K, Hall AJ, Lorenti ED, Sellergren B (2001) Target analogue imprinted polymers with affinity for folic acid and related compounds. *J Am Chem Soc* 123(10):2146–2154
24. He LM, Su YJ, Zheng YQ, Huang XH, Wu L, Liu YH, Zeng ZL, Chen ZL (2009) Novel cyromazine imprinted polymer applied to the solid-phase extraction of melamine from feed and milk samples. *J Chromatogr A* 1216(34):6196–6203
25. Song XL, Li JH, Wang JT, Chen LX (2009) Quercetin molecularly imprinted polymers: preparation, recognition characteristics and properties as sorbent for solid-phase extraction. *Talanta* 80(2):694–702
26. Pakade V, Lindahl S, Chimuka L, Turner C (2012) Molecularly imprinted polymers targeting quercetin in high-temperature aqueous solutions. *J Chromatogr A* 1230(23):15–23
27. Ban L, Han X, Wang XH, Huang YP, Liu ZS (2013) Carprofen-imprinted monolith prepared by reversible addition-fragmentation chain transfer polymerization in room temperature ionic liquid. *Anal Bioanal Chem* 405(26):8597–8605
28. Holland N, Frisby J, Owens E, Hughes H, Duggan P, McLoughlin P (2010) The influence of polymer morphology on the performance of molecularly imprinted polymers. *Polymer* 51(7):1578–1584
29. Dauwe C, Sellergren B (1996) Influence of template basicity and hydrophobicity on the molecularly recognition properties of molecularly imprinted polymers. *J Chromatogr A* 753(2):191–200
30. Gavazzini A, Marchetti N, Guzzinati R, Pasti L, Ciogli A, Gasprini F, Lagana A (2014) Understanding mixed-mode retention mechanisms in liquid chromatography with hydrophobic stationary phase. *Anal Chem* 86(10):4919–4926
31. Zhong DD, Huang YP, Xin XL, Liu ZS, Aisa HA (2013) Preparation of metallic pivot-based imprinted monolith for polar template. *J Chromatogr B* 934(1):109–116
32. Bian M, Zhang Z, Yin H (2012) Effects and mechanism characterization of ionic liquids as mobile phase additives for the separation of matrine-type alkaloids by liquid chromatography. *J Pharm Biomed* 58(25):163–167
33. Zhang YG, Song D, Lanni L, Shimizu K (2010) Importance of functional monomer dimerization in the molecular imprinting process. *Macromolecules* 43(15):6284–6294
34. Caro E, Masque N, Mzcre RM, Borrul F, Comack PAG, Sherrington DC (2002) Non-covalent and semi-covalent molecularly imprinted polymers for selective on-line solid-phase extraction of 4-nitrophenol from water samples. *J Chromatogr A* 963(1–2):169–178
35. Yang CX, Liu SS, Wang HF, Wang SW, Yan XP (2012) High-performance liquid chromatographic separation of position isomers using metal-organic framework MIL-53(Al) as the stationary phase. *Analyst* 137(1):133–139
36. Kaszynska MS, Jaszczolt K, Witt D, Rachon J (2004) High-performance liquid chromatography of di- and trisubstituted aromatic positional isomers on 1,3-alternate 25,27-dipropoxy-26,28-bis-[3-propyloxy]-calix[4] arene-bonded silica gel stationary phase. *J Chromatogr A* 1055(1–2):21–28
37. Sellergren B, Shea KJ (1995) Origin of peak asymmetry and the effect of temperature on solute retention in enantiomer separations on imprinted chiral stationary phases. *J Chromatogr A* 690(1):29–39
38. Denderz N, Lehotay J, Cizmarik J, Cibulkova Z, Simon P (2012) Thermodynamic study of molecularly imprinted polymer used as the stationary phase in high performance liquid chromatography. *J Chromatogr A* 1235(27):77–83
39. Dender N, Lehotay J (2012) Application of the Van't Hoff dependences in the characterization of molecularly imprinted polymers for some phenolic acids. *J Chromatogr A* 1268(14):44–52
40. Kim H, Kaczmarek K, Guiochon G (2006) Thermodynamic analysis of the heterogeneous binding sites of molecularly imprinted polymers. *J Chromatogr A* 1101(1–2):136–152
41. Kim H, Guiochon G (2005) Thermodynamic functions and intraparticle mass transfer kinetics of structural analogues of a template on molecularly imprinted polymers in liquid chromatography. *J Chromatogr A* 1097(1–2):84–97
42. Liu YQ, Hoshina K, Haginaka J (2010) Monodispersed, molecularly imprinted polymers for cinchonidine by precipitation polymerization. *Talanta* 80(5):1713–1718